2014

QPCR analysis of functional genes in iron-rich microbial mats at an active hydrothermal vent system Loihi Seamount, Hawaii

Kelsey J. Jesser
Western Washington University

QPCR ANALYSIS OF FUNCTIONAL GENES IN IRON-RICH MICROBIAL MATS AT AN ACTIVE HYDROTHERMAL VENT SYSTEM LOIHI SEAMOUNT, HAWAII

By

Kelsey J. Jesser

Accepted in Partial Completion
Of the Requirements for the Degree
Master of Science

Kathleen L. Kitto, Dean of the Graduate School

ADVISORY COMMITTEE

Chair, Dr. Craig L. Moyer

Dr. Marion Brodhagen

Dr. Dietmar Schwarz

MASTER'S THESIS

In presenting this thesis in partial fulfillment of the requirements for a master's degree at Western Washington University, I grant to Western Washington University the non-exclusive royalty-free right to archive, reproduce, distribute, and display the thesis in any and all forms, including electronic format, via any digital library mechanisms maintained by WWU.

I represent and warrant this is my original work, and does not infringe or violate any rights of others. I warrant that I have obtained written permissions from the owner of any third party copyrighted material included in these files.

I acknowledge that I retain ownership rights to the copyright of this work, including but not limited to the right to use all or part of this work in future works, such as articles or books.

Library users are granted permission for individual, research and non-commercial reproduction of this work for educational purposes only. Any further digital posting of this document requires specific permission from the author.

Any copying or publication of this thesis for commercial purposes, or for financial gain, is not allowed without my written permission.

Kelsey Jesser

July 2014

QPCR ANALYSIS OF FUNCTIONAL GENES IN IRON-RICH MICROBIAL MATS AT AN ACTIVE HYDROTHERMAL VENT SYSTEM LOIHI SEAMOUNT, HAWAII

A Thesis
Presented to
The Faculty of
Western Washington University

In Partial Fulfillment
Of the Requirements for the Degree
Master of Science

By
Kelsey Jesser
July, 2014

ABSTRACT

The recently discovered *Zetaproteobacteria* represent a novel class of *Proteobacteria* which oxidize Fe(II) to Fe(III), driving CO_2 fixation at hydrothermal vents. These chemolithoautotrophs are the dominant bacterial population in iron-rich microbial mats, and represent a unique opportunity to investigate the connection between deep-sea geochemical processes and the dark microbial world. *Zetaproteobacteria* were first discovered at Loihi Seamount, located 35 km southeast off the big island of Hawaii and characterized by low-temperature diffuse hydrothermal venting. These vents are surrounded by luxuriant, iron-rich microbial mats that are colonized and often dominated by *Zetaproteobacteria*. Five novel non-degenerate QPCR assays were designed using sequence data derived from microbial iron-mat samples collected at Loihi in March 2013. Genes of interest were *nifH*, *nirK*, and *arsC*, associated with microbial nitrogen fixation, denitrification and arsenic detoxification, respectively. We also examined carbon fixation genes *cbbM* and *aclB*, which are indicators for the Calvin Benson Bassham (CBB) and reductive tricarboxylic acid (rTCA) cycles, respectively. All functional genes were found to be present at Loihi Seamount with the exception of *nifH*, which was undetectable with our method. Functional genes *arsC* and *nirK* were detected in all samples assayed, indicating that both arsenic detoxification and denitrification processes are likely occurring across all hydrothermal mat habitats. *cbbM* and *aclB* were also detectable in all samples assayed, indicating the co-occurence of these two modes of carbon fixation. T-RFLP analysis indicates that the communities in iron-rch mat samples collected in 2013 are very similar to one another. T-RFLP Group 1 had high *Zetaproteobacteria* abundance and low *aclB* relative to *cbbM*, indicating that the CBB cycle is the major mode of carbon fixation in *Zetaproteobacteria*-rich mat communities. T-RFLP Group 2 had low *Zetaproteobacteria* abundance and high *aclB* gene copy numbers, suggesting that the rTCA cycle is operating in non-*Zetaproteobacteria* taxa and plays an important role in carbon fixation in these communities. Based on these results, we conclude that *aclB* may be an important functional gene indicator of community composition. QPCR variance was explained by mat morphology but not temperature or sample site. Gene *aclB* was significantly associated with mat morphology, and may contribute to the significant relationship between the QPCR data and mat type. Fe(II) was significant with mat morphology. Geochemistry data was significantly associated with sample site and mat morphology, indicating that there is a range of chemistries in which these iron-rich microbial communities can thrive, and/or that the abundance of functional genes in these mat communities changes gradually in response to more dynamic chemical variation over time. Together, these QPCR assays constitute a 'functional gene signature' for iron mat samples across a broad array of temperatures, mat types, chemistries, and sampling sites in and around Pele's Pit at Loihi Seamount.

ACKNOWLEDGEMENTS

I would like to express my thanks and appreciation to my adviser, Dr. Craig Moyer, for his wisdom, encouragement, and the many opportunities he provided me as a member of his research group. I would also like to thank my committee members Dr. Marion Brodhagen and Dr. Dietmar Schwarz. Their help and expertise over the course of this project has been invaluable. I am grateful to my fellow lab members, especially to Dr. Heather Fullerton for assembling and helping to interpret the metagenomic data used to develop the assays reported herein, and to Kevin Hager who ran and analyzed the T-RFLP DNA fingerprinting data for this project. I would like to acknowledge the collaboration of Dr. Brian Glazer and Dr. Jason Sylvan and thank them for allowing me access to their chemical data for Loihi Seamount. Many thanks to the scientists and crew onboard the *R/V Thomas G. Thompson* during our March 2013 research cruise and to the pilots of the *ROV Jason II*, all of whom were instrumental in helping to gather samples for this project. This work was funded by WWU's Office of Research and Sponsored Programs, Biology Alumni Student Research Fellowship and grants from the National Science Foundation. I am also grateful for the support my fellow graduate students, and the WWU biology faculty and staff.

TABLE OF CONTENTS

LIST OF FIGURES

LIST OF TABLES

INTRODUCTION

Deep-sea hydrothermal vents are dynamic and extremely productive biological ecosystems supported by chemosynthetic microbial primary production. In the absence of photosynthesis, microorganisms derive energy via the oxidation of reduced chemicals (such as H_2, H_2S, Fe(II), and CH_4) emitted in hydrothermal fluids (Jannasch and Mottl, 1985). In contrast to other strategies for microbial chemosynthesis at hydrothermal vents, iron oxidation has only more recently been studied (Emerson and Moyer, 2002). By weight, iron is the most abundant element in the earth, and has vast potential as an energy source for microbes via chemolithoautotrophy coupled to Fe(II) oxidation (Hedrich et al., 2011). However, iron's ability to act as an electron donor for the biotic fixation of CO_2 in neutrophilic environments is limited by the rapid abiotic oxidation of Fe(II) to Fe(III) in the presence of oxygen (Druschel et al., 2008; Weber et al., 2006). Despite the ephemeral nature of iron as an energy source, iron-oxidizing bacteria (FeOB) have been identified in a wide array of freshwater and marine habitats, and can flourish at circumneutral deep-sea vents with sharp redox gradients and hydrothermal fluids high in CO_2 and reduced iron (Emerson et al., 2007; Glazer and Rouxel, 2009; Holland, 2006; Soblev et al., 2004). The recently described *Zetaproteobacteria* represent a novel class of marine *Proteobacteria* that are diverse and abundant contributors to deep-sea FeOB communities (Emerson and Moyer, 2010).

Zetaproteobacteria were first discovered at iron-rich low-temperature hydrothermal vents at Loihi Seamount, Hawaii (Emerson and Moyer, 2002) and have been demonstrated to be significant microbial colonizers of seamounts (Emerson and Moyer, 2010; Rassa et. al 2009). Loihi Seamount is a seismically active submarine hotspot volcano approximately 35

km southeast of the big island of Hawaii. It is the youngest seamount of the Hawaiian island chain and actively emits Fe(II) and CO_2-rich hydrothermal vent effluent, which supports luxuriant rust-colored mats formed during microbial iron oxidation (Emerson and Moyer, 2010; Glazer and Rouxel, 2009; Sakai et al., 1987). In 1996 a major eruption event occurred at Loihi and formed Pele's Pit (Fig. 1), a 300m caldera near the summit with several active hydrothermal venting sites (Dunnebier et al., 1997).

The *Zetaproteobacteria* to have a relatively high phenotypic diversity, yet only a single species, *Mariprofundus ferrooxydans*, has been described thus far (Emerson et al., 2007; McAllister et al., 2011; Singer et al., 2011). *M. ferrooxydans* is a chemolithoautotrophic microaerophilic FeOB, with few genomic similarities to other hydrothermal vent *Proteobacteria* or other well-characterized freshwater iron-oxidizers (Singer et al., 2011). There is compelling evidence to suggest that additional phylogenetic and functional diversity may exist within the *Zetaproteobacteria*, as shown by McAllister et al. (2011).This study analyzed a number of iron-rich microbial biomes in a global survey of SSU rDNA sequences, and identified 28 unique operational taxonomic units (OTUs) based on 97% minimum sequence similarity. Of these, 13 OTUs were endemic to a specific region and 2 were found to be ubiquitous throughout the Pacific Ocean. *M. ferrooxydans* was not represented in any of these cosmopolitan OTUs, suggesting that *Mariprofundus* sp. strains may be a comparatively minor lineage of *Zetaproteobacteria* from an ecological perspective (Emerson and Moyer, 2010).

While McAllister et al. (2011) described the biogeography and phylogenetic diversity of *Zetaproteobacteria*, little is known about how this diversity may translate to functional and/or morphological variations across deep-sea hydrothermal vent habitats and microbial

communities. In addition to the *Zetaproteobacteria*, bacterial clone library analysis has identified several other members of the microbial communities at Loihi. Consistently observed counterpart microorganisms include members of the *Gammaproteobacteria*, *Deltaproteobacteria*, *Epsilonproteobacteria*, and *Chloroflexi* (Flemming et al., 2013; McAllister et al., 2011). The presence of these diverse taxa suggests great metabolic and functional diversity may exist within *Zetaproteobacteria*-dominated microbial mat communities.

Both marine and freshwater FeOB secrete filamentous Fe(III)-oxyhydroxides during iron oxidation. FeOB likely produce these structures in order to avoid encrustation as Fe(II) is oxidized to insoluble Fe(III) at circumneutral pH (pH 5.5-7.4). These distinctive secretions are instrumental in the formation of microbial iron mats supplied by Fe(II)-rich vent fluids, and are thought to be important in determining fluid flow, dispersion, colonization, and biotic geochemical cycling throughout the ecosystem (Chan et al., 2011). Distinct mat morphologies associated with varying forms of Fe(III)-oxyhydroxides (e.g. tubular sheaths vs. twisted helical stalks) have been consistently observed at Loihi. Fine-scale microscopy and terminal-restriction length polymorphism (T-RFLP) analyses of distinct mat morphotypes (Flemming et al., 2013) provide evidence that various mat types may represent phylogenetically distinct distributions of microbial populations. We hypothesized that this variation in iron mat morphology and community structure would translate into unique metabolic and functional signatures.

This study describes the use of five novel, non-degenerate quantitative PCR (QPCR) assays to estimate key functional gene sequences for carbon and nitrogen fixation, denitrification, and arsenic detoxification in *Zetaproteobacteria*-rich microbial mat

communities at Loihi Seamount, Hawaii. The goal of this research was to use QPCR in conjunction with chemical analyses and T-RFLP DNA fingerprinting to analyze microbial mat samples across a range of environmental parameters. Previous studies have used QPCR to quantify functional genes at hydrothermal vents and in other microbial biomes. Wang et al. (2009) used QPCR data to verify a GeoChip analysis of functional genes in microbial communities at the Juan de Fuca Ridge hydrothermal vent system. QPCR has also been utilized to study denitrification in soils (Sonia et al., 2004), sulfate-reduction in a solid-waste digestor (Tang et al. 2004), pollutant degrader genes (Beller et al., 2002; Kikuchi et al., 2002), and in many other functional capacities in a wide array of microbial communities and habitats. However, many of these studies have utilized degenerate primers designed using sequence data from databases and other sources. Our unique approach to non-degenerate primer design for QPCR using sequence data for samples collected from these iron-rich microbial mats has enabled us to quantify an array functional genes specific to these habitats and communities. Little is known about mineral cycling in the *Zetaproteobacteria* habitats at Loihi, and this work constitutes the first effort to develop a non-degenerate QPCR approach to functional gene analysis in deep-sea FeOB-rich communities.

METHODS

Sampling for T-RFLP and QPCR

Microbial iron mat samples were collected within Pele's Pit hydrothermal venting sites Hiolo North (Markers 31, 36, 39), Hiolo South (Markers 34, 38), and on the caldera rim at Pohaku (Marker 57) at Loihi Seamount, Hawaii (Fig. 1). Samples were collected using a biomat syringe (BMS) sampler, a custom-designed tool for fine-scale microbial mat sampling (Breier et al., 2012). The BMS sampler was operated by the *ROV Jason II* from the *R/V Thomas G. Thompson* during a March 2013 cruise to Loihi. Gross mat morphology was assigned based on consistently observed iron mat morphotypes at these sites (Fig. 2). Sample names reflect ROV dive number (e.g., 671-676), sample type and number (e.g., BMS1-3), and the sampler and syringes used (e.g., samplers A-D, syringes 1-6). Mat samples were brought onboard and either directly frozen at -80˚C or extracted for genomic DNA (gDNA). For comparison, a single scoop sample, PV340, was analyzed. Scoop sample PV340 was collected in 1997 using the submersible *DSRV Pisces V* at Jet Vents (Marker 11), which is now dormant. This mat community was not indicative of an FeOB-dominated mat community, but rather contained only a few populations of known sulfur-cycling *Epsilonproteobacteria* (Emerson and Moyer 2010).

gDNA extraction

Genomic DNA (gDNA) was extracted using the Fast DNA SPIN kit for soil (Qbiogene, Carlsbad, CA) according to the manufacturer's protocol. A FastPrep instrument (Qbiogene) was used at speed 5.5 for 30 s to optimize cellular lysis, and gDNA was eluted in 10 mM Tris at pH 8.0. A NanoDrop ND-1000 spectrophotometer was used to determine the purity and concentration of all nucleic acid samples.

Metagenomic sequencing and assembly

Syringe sample J2-470-BS3 (81.8% *Zetaproteobacteria* by QPCR) was collected from a microbial iron mat at Pohaku (Fig. 1) on the 2009 using the *ROV Jason II*. Scoop sample SB13 (13% *Zetaproteobacteria*) was directly collected from an intertidal microbial iron mat at Site 13, Soda Bay, Alaska in a 50 mL centrifuge tube and immediately preserved with RNA later. The HiSeq Illumina platform was used to sequence gDNA from these samples. Illumina reads were assembled using MetaVelvet, a freeware short-read assembler for metagenomics (Namiki et al., 2012). Genes of interest were identified using MG-RAST annotations of metagenome assemblies (Meyer et al., 2008).

Primer design

Non-degenerate QPCR primers for arsenate reductase (*arsC*) and nitrite reductase (*nirK*) were designed using annotated functional gene sequences from our Pohaku (J2-479-BS3) metagenomic assembly. These genes are associated with arsenic detoxification and denitrification, respectively (Braker et al., 2000; Mukhopadhyay and Rosen, 2002). Nitrogenase (*nifH*) primers were based on an annotated functional gene sequence from the Soda Bay (Site 13; SB13) metagenomic assembly. *nifH* is an indicator gene for microbial nitrogen fixation (Gaby and Buckley et al., 2012; Mehta et al., 2002).

Non-degenerate QPCR primers were designed for carbon fixation genes using PCR-cloned sequences. PCR primers for ribulose-1,5-bisphosphate carboxylase (RuBisCO) type II (*cbbM*) were first obtained from Kato et al. (2012). RuBisCO is associated with carbon fixation via the Calvin Benson Bassham (CBB) cycle (Tabita et al., 2007). Primers from Campbell et al. (2003) were used to amplify ATP citrate lyase (*aclB*), an important gene for carbon fixation via the reductive tricarboxylic acid (rTCA) cycle. These degenerate primer

sets for *cbbM* and *aclB* were then used to amplify and sequence PCR products from BMS samples collected at Loihi in March 2013. Sequence data for PCR cloned amplicons were used to generate non-degenerate nested primer sets for QPCR that are specific for the microbial communities at Loihi. All functional gene primer sequences and sources are summarized in Table 1.

Cloning for QPCR standards

Linearized plasmid standards for all functional gene analyses were constructed via PCR. PCRs were optimized for 3 ng gDNA template using a reaction mixture of 1 µM (each) forward and reverse primer, 2.5 mM MgCl, 1 µM Taq, 1X PCR buffer, 10 ug BSA, and 200 µM of each dinucleoside triphosphate. PCR conditions were as follows: initial 2-minute hot start at 94˚C, 35 cycles of denaturation (94˚C for 1 min), annealing (50-60˚C for 90 seconds), and elongation (72˚C for 3 min), and a final elongation step at 72˚C for 3 min. Annealing temperature varied for each primer set as outlined in Table 1. No template controls were maintained for each PCR run. Amplified products were examined against the 1-kb DNA ladder (New England Biolabs, Ipswich, MA) using 2% agarose gel electrophoresis to determine size and specificity of the amplicon for each primer set. PCR reactions were purified using the QIAEX II gel extraction kit (Qiagen, Valencia, CA) according to the manufacturer's protocol for desalting and concentrating DNA solutions.

PCR amplicons were then cloned into the pCR4-TOPO *E. coli* vector using the TOPO TA cloning kit for sequencing with One Shot TOP10 chemically competent cells according to the manufacturer's instructions (Life Technologies, Carlsbad, CA). Randomly selected colonies were streaked to isolation and grown in 5 mL LB broth medium in a shaking incubator at 200 rpm for 24h at 37˚C. Plasmids were extracted and purified from cloned cells

using the QIAprep miniprep system (Qiagen) and PCR screened for correct insert size using the M13F and M13R primers (Moyer, 2001). Plasmid amplicons were checked against a 1kb ladder using 2% gel electrophoresis to ensure correct insert size.

Cloned amplicons were sequenced in both directions with M13F and M13R primers on an ABI 3130xl genetic analyzer (Life Technologies). Forward and reverse sequences were aligned and trimmed using BioNumerics v.7.1 (Applied Maths, Saint-Martens-Latem, Belgium). Nucleotide sequences were checked using multiple sequence alignments to confirm that the sequence of the cloned vector insert was correct and that primers were targeting desired functional gene sequences for all cloned amplicons. Plasmids were linearized using the restriction enzyme *NotI* (New England Biolabs).

Functional gene QPCR

Functional genes were quantified using absolute quantitation for gDNA against linearized plasmid standards. All QPCR assays were run in a 96 well plate format on a Step One Plus Real Time PCR System (Life Technologies). Samples were run in triplicate using 2X Power SYBR Green Mastermix (Life Technologies). For all assays, 0.3 µM each forward and reverse primer was used in a total reaction volume of 20 µL. One nanogram gDNA template was run for each unknown sample using absolute quantitation against a 10-fold dilution series of one nanogram linearized plasmid (10^{-1}-10^{-7}). Samples were run in triplicate alongside negative controls at 95˚C for 10 min (initial denaturation), and 40 cycles of 95˚C for 15 seconds (denaturation) and 50-60˚C for 1 min (annealing). Annealing temperature for each functional gene primer set is summarized in Table 1. Melt curve analysis was performed after each assay to check PCR specificity. QPCR outputs were manually checked to ensure that default baseline and threshold settings were correct and consistent across all plates.

Standard curves and linear regression data for each assay were calculated, as well as standard deviation for each range of cross threshold (C_t) values produced. Gene copy number per nanogram gDNA was determined based on the size of the linearized plasmid used as the QPCR standard (Ritalahti et al., 2006). A nonparametric Kruskal-Wallis one-way analysis of variance (ANOVA) was run for all functional gene QPCR data using the program SigmaPlot v.12.5 (Systat Software, San Jose, CA)

A non-parametric multidimensional scaling (NMDS) plot was created between variables for log-transformed functional gene QPCR data and *Zetaproteobacteria* abundance QPCR data using a Pearson product correlation resemblance matrix using Primer v6 (Clarke and Gorley, 2006). *nifH* gene amplification was low or undetectable by our method and was not included in the NMDS plot.

Zetaproteobacteria QPCR

Nearly complete *Zetaproteobacteria* SSU rRNA gene sequences from the NCBI database were aligned with the SILVA SINA web aligner (Pruesse et al., 2007) and imported into the SILVA 102 NR database operated by the ARB sequence program (Ludwig et al., 2004). *Zetaproteobacteria*-specific QPCR primers Zeta542F (GAA AGG DGC AAG CGT TGT T) and Zeta658 (TGC TAC ACD CGG AAT TCC GC) were built using the PROBE MATCH tool. Total bacterial SSU rRNA copies were quantified with bacterial primers Bact533F (GTG CCA GCA GCC GCG GTA A) and Bact684R (TCT ACG SAT TTY ACY SCT AC).

QPCR conditions were as described for functional genes with an annealing temperature of 60˚C. Percent *Zetaproteobacteria* were calculated by dividing

Zetaproteobacteria gene copy numbers per nanogram gDNA by copy numbers calculated against the bacteria-specific primer set.

Chemistry and temperature measurements

End-member hydrothermal fluids were collected from chimneys and microbial mats using a titanium major sampler deployed from the *ROV* Jason II (Von Damm et al., 1985). Background samples were collected away from venting sites using Niskin bottles attached to the side of *ROV* Jason II. Hydrothermal fluid samples were filtered through 0.2 μm polycarbonate filters and then frozen immediately.

Fluid temperatures were measured using the temperature probe on *ROV* Jason II. NO_x was measured using the chemiluminescent method with a NO_x box, which has a detection limit of <0.010 μM NO_x (Garside et al., 1982). NH_4^+ was measured using the fluorescence method (Holmes et al., 1999) post-cruise. The detection limit for NH_4^+ is 0.030 μM. Dissolved inorganic phosphorus (P_i) and dissolved silica (mostly silicate, dSi) were measured using colorimetric methods, with a detection limit of 0.030 μM P_i and 0.30 μM for dSi (Grasshoff et al., 1999). Fe(II) concentrations in mat samples were determined using the ferrozine method with a detection limit of <1 μM (Stookey et al., 1970).

T-RFLP DNA Fingerprinting

T-RFLP was completed as described by Flemming et al. (2013). Triplicate PCR reactions with a 5' end-labeled 6-FAM fluorescent dye were pooled, concentrated, and diluted in Tris buffer. PCR products were equally divided between eight overnight restriction digest treatments: *AluI, BstUI, HaeIII, HhaI, HinfI, MboI, MspI,* and *RsaI* (New England BioLabs). All reactions were run at 37˚C, with the exception of *BstUI,* which was incubated at 60˚C. The restriction fragments were desalted with Sephadex G-75 (Amersham

Biosciences, Uppsala, Sweden) and dried down. Fragments were rehydrated in 15 µL of a 1/30 solution of LIZ-500 internal size standard in formamide. Reactions were denatured at 95˚C for ten minutes and separated via capillary electrophoresis using an ABI 3130x1 genetic analyzer with 50-cm capillary array and POP-6 polymer (Life Technologies). Electropherograms were imported into BioNumerics v.7.1 (Applied Maths) and sized against the internal standard. Only fragments between 50 and 500 bp were included in the analysis. Community fingerprints were compared using average Pearson product moment correlation and unweighted pair group method with arithmetic mean (UPGMA) cluster analysis for all eight digests using the relative fluorescent proportions of each electropherogram. Cophenetic correlation coefficient values were calculated for all nodes with 3 or more branches. All T-RFLP analyses were performed in BioNumerics as previously described.

Statistical Analyses

Four non-parametric one-way multivariate analyses of variance (MANOVA) were run for QPCR gene abundance numbers (*cbbM, aclB, arsC, nirK, nifH*) for the following independent variables: mat morphology, temperature range (10˚C intervals), percent *Zetaproteobacteria* range (5-10% intervals), and sample site. Three one-way MANOVA were run for chemistry data with the independent variables of mat morphology, temperature range, and sample site. Wilke's lambda p-values below 0.05 were considered statistically significant. For significant results, test between subjects effects (univariate ANOVA) results were examined to determine which variables were statistically significant for a given independent variable ($p<0.05$). These analyses were completed using the statistical software SPSS v.17 (IBM, Armonk, NY).

RESULTS

QPCR analysis for 17 Loihi 2013 BMS samples across various mat morphologies, vent effluent and mat temperatures, fluid chemistries, and sample sites revealed unique functional gene signatures for each fine-scale microbial mat community sampled by the biomat syringe (BMS) sampler (Fig. 3). There was substantial variation in functional gene abundances across communities. Overall, Calvin Benson Bassham (CBB) carbon fixation gene *cbbM* was the most abundant gene sequence per ng DNA, followed by *arsC*, *nirK*, and *aclB*, based on cumulative averages. Gene copy numbers for *nifH* were either very low or undetectable by our method. Two mat samples from Hiolo South (675-BM2-A123 and 675-BM1-A123) had relatively higher numbers of *arsC*. Pohaku sample 674-BM2-D12456 had the greatest number of cumulative gene copy numbers across the five QPCR assays ($>10^7$). Hiolo North sample 672-BM1-B123456 had the fewest gene copy numbers ($<10^3$) and had high *aclB* gene copies per ng gDNA relative to the other mat samples. Nonparametric Kruskal-Wallis one-way ANOVA showed that differences in the median abundance between functional genes was greater than would be expected by chance ($p<0.001$). The non-parametric multidimensional scaling plot (NMDS) (Fig. 4) for QPCR functional gene variables and for *Zetaproteobacteria* abundance clustered *cbbM, nirK*, and *arsC* with >60% Pearson correlation coefficient similarity. This group was also associated with *Zetaproteobacteria* abundance. *aclB* did not group with any other QPCR variable.

T-RFLP DNA fingerprinting (Fig. 5A) revealed that the microbial communities at hydrothermal vents near the summit region of Loihi Seamount were very similar to each other (>40% similarity between samples). T-RFLP clusters were assigned membership in two distinct groups. T-RFLP Group 1 had 33% *Zetaproteobacteria* on average and low *aclB*

abundance relative to Group 2. T-RFLP Group 2 had 9.1% *Zetaproteobacteria*, much higher *aclB*, and was grouped more closely with the comparator sample PV340. Pohaku BMS samples were all clustered in T-RFLP Group 1. Hiolo North and Hiolo South samples formed distinct clusters within Group 1 according to vent type and temperature, though 672-BM1-D123456, a Hiolo North curd-like mat, grouped more closely with the Pohaku mat samples. Two veil-type samples from different sites (672-BM1-B12345 and 672-BM2-A56C456) clustered tightly with >80% similarity in the community fingerprint analysis. Group 2 was comprised of Hiolo South samples 675-BM3-D12346 (surface mat; 48.1˚C) and 676-BM2-C34 (streamers; 33.1˚C).

Functional gene data for key carbon fixation enzymes *aclB* (Fig. 5B) and *cbbM* (Fig. 5C) are compared with the T-RFLP community analysis (Fig. 5A). Jet Vents scoop sample PV340 had very high *aclB* gene copy numbers relative to the Loihi 2013 samples. Group 2 was most closely associated with PV340, and overall Group 2 samples had high *aclB* gene copy numbers compared to Group 1. Group 1 T-RFLP samples had the highest average percent *Zetaproteobacteria* (33%) by QPCR. Group 2 T-RFLP samples had substantially lower numbers of *Zetaproteobacteria* (9.1%). *Zetaproteobacteria* were only just detectable in PV340 (0.21%). Both PV340 and 676-BM2-C34 are classified as ‘streamers’, filament-like bits of mat in actively venting orifices (Fig. 2B). In general, samples low in *aclB* generally had much higher *cbbM*. *cbbM* was ubiquitous in all samples, regardless of where they were in the T-RFLP cluster analysis, though it is interesting to note that 674-BM2-D12456 (Group 1) had exceptionally high *cbbM*.

One-way MANOVA for functional gene QPCR data indicated that mat morphology was a significant factor for QPCR variance across samples ($p<0.0005$). Temperature, sample

site and percent *Zetaproteobacteria* did not significantly describe the QPCR data. Univariate ANOVA revealed that *aclB* gene copy numbers were significantly explained by changes in mat type ($p<0.0005$). Functional gene abundances for *cbbM*, *arsC*, *nirK*, and *nifH* were not significantly associated with mat morphology.

Geochemical measurements were collected for 14 of our 17 Loihi BMS samples. Mat morphology and sample site showed a significant effect with vent chemistry (one-way MANOVA, $p<0.0005$ for both). Univariate ANOVA showed that Fe(II) levels were significant with mat type ($p=0.003$), and that NH_4, NO_x, dSI, and PO_4 were significant with sample site ($p=0.019$, 0.03, 0.001, <0.0005, respectively). Mat temperature was not significant with any chemistry measure (one-way MANOVA, $p=0.087$).

DISCUSSION

These novel QPCR assays were designed to target annotated gene sequences from microbial mat communities living around the vents at Loihi Seamount, but may also be useful in similar iron-dominated hydrothermal systems. Because our primers were designed to be non-degenerate, we have enhanced confidence in the sequence identity of our PCR amplicons. We are reporting on the amplification of functional gene via primers designed to target sequences unambiguously identified in communities dominated by iron-oxidizing bacteria (FeOB) at our study sites. Most QPCR approaches to functional gene amplification in environmental samples have utilized degenerate primers, and have largely focused on the amplification of one or two genes associated with a single pathway or group of organisms (Agrawal and Lal, 2009; Church et al., 2005; Henry et al., 2004). Use of degenerate primers increases the risk of non-specific amplification, largely due to primer bias as primers not used during amplification are available to prime non-specific sites (Rose et al. 1998). As QPCR is an exceptionally sensitive molecular tool, we chose to be conservative in our strategy for probe design, using either annotated metagenomic functional gene sequences or cloned sequence representatives of microbial mat communities present at Loihi to design primers (Table 1).

Sequencing and QPCR detection of an arsenic reductase (*arsC*) gene sequence comprises the first look at an arsenic detoxification gene in the microbial communities supported by the hydrothermal vents in and around Pele's Pit. Bacterial arsenic resistance/detoxification is conferred by *arsC*. This enzyme catalyzes the intracellular reduction of arsenate to arsenite, which is then extruded from the cell via an arsenite-specific protein pump (Jackson and Dugas, 2003; Mukopadhyay and Rosen, 2002). The results of this

study indicate that *arsC* is present and quantifiable in all iron-rich mat communities assayed (Fig. 3). Though there is presently no data on arsenate/arsenite chemistry at Loihi or other *Zetaproteobacteria*-rich venting sites, Meyer-Dombard et al. found both *arsC* and *Zetaproteobacteria* SSU gene sequences in vent fluids and colonized slide community experiments in arsenic-rich waters at shallow hydrothermal vents at Tutum Bay, Papua New Guinea (2012). We identified several samples high in *arsC* that are intriguing candidates for continued investigations into the presence and expression of arsenic cycling genes. Samples 675-BM2-A123, and 675-BM1-A123 had exceptionally high *arsC* relative to the other Loihi 2013 mat communities analyzed. These samples were both collected at Hiolo South and came from microbial mats that were >40˚C.

We developed a new QPCR assay to quantify nitrogenase (*nifH*) identified in a *Zetaproteobacteria*-rich iron cold seep at Soda Bay, Alaska. Biological fixation of nitrogen gas occurs via nitrogenase. *nifH*, which encodes the nitrogenase reductase subunit, is the most commonly used molecular marker for microbial nitrogen fixation (Gaby and Buckley et al., 2012). *nifH* sequence abundance was either very low or undetectable in the samples analyzed and was not present in the Pohaku metagenomic assembly. This assay may be best suited to the amplification of *nifH* from iron mats exposed to sunlight and undergoing photosynthesis in addition to chemosynthesis, such as those in the iron-rich cold seeps at Soda Bay. However, based on the absence of an annotated gene sequence in the metagenomic assembly from Pohaku Vents and the negligible QPCR amplification of *nifH* using a wide array of both degenerate and non-degenerate primer sets (data not shown), it is possible that nitrogen fixation via the *nifH* subunit of nitrogenase is not an important function

of hydrothermal iron-based microbial mat communities. Additional investigations into the presence and expression of *nif* genes are needed to confirm this hypothesis.

The presence of a dissimilatory copper-containing nitrite reductase (*nirK*) at Loihi is suggestive of denitrifying activity (Fig. 3). Often used as a molecular probe for microbial denitrification, the enzyme products of *nir* enzymes are responsible for reducing a mineralized form of nitrogen to gas through the reduction of nitrite to NO (Bothe et al., 2000; Braker et al., 1998; Braker et al., 2000; Smith et al., 1992). Though previous studies have identified denitrification genes at hydrothermal vents (Wang et al., 2009; Xie et al., 2011), they were only recently detected at Loihi and in the *Zetaproteobacteria* via an annotated metagenomic assembly of a fosmid library (Singer et al., 2013). *nirK* was amplified by QPCR in all samples described here, confirming the presence of denitrification genes in a wide array of iron mat communities. The presence of *nirK* is notable as nitrite reduction may open up new ecological niches for these organisms within iron-rich microbial mat habitats with nitrogen oxides acting as electron acceptors in anoxic mat environments.

The Calvin Benson Bassham (CBB) cycle is thought to be the most prevalent mode of carbon fixation on earth and has been identified at hydrothermal vents (Nakagawa and Takai, 2008). Ribulose-1,5-bisphosphate carboxylase (RuBisCO) enzymes catalyze the carboxylation of ribulose-1,5-bisphosphate with CO_2 in the essential step of the CBB cycle. RuBisCOs are organized into four groups, with RuBisCO type I (*cbbL*) and RuBisCO type II (*cbbM*) most often identified in deep-sea chemolithoautotrophs (Minic and Thongbam, 2011; Nakagawa and Takai, 2008; Shively et al., 1998). RuBisCO types I and II are used by hydrothermal vent microbes under varying oxygen and carbon dioxide conditions. A dimer of large subunits, *cbbM* is considered most effective in higher carbon dioxide environments

(Tabita et al., 2007). High levels of CO_2 (>300 mM) have been detected in vent effluents at Loihi (Wheat et al., 2000), and metagenomic assemblies (data not shown) from Loihi mats have found that *cbbM* is much more prevalent than *cbbL*. The ubiquity of *cbbM* in the 17 fine-scale mat communities collected with the BMS sampler and assayed herein (Fig. 3; Fig. 5C) suggests that the CBB cycle via *cbbM* is likely the most important mode of carbon fixation in this habitat. Both *cbbL* and *cbbM* have been identified in *M. ferrooxydans* (Emerson et al., 2007; Singer et al., 2011). Though the presence of a gene is not a guarantee of activity, the discovery of considerably more *cbbM* sequences relative to *cbbL* in metagenomic studies at Loihi may indicate that *M. ferrooxydans* is not an ecologically suitable representative of the *Zetaproteobacteria* that act as ecosystem engineers in these iron-mat ecosystems, as suggested by Emerson and Moyer (2010). Future culturing endeavors should focus on those communities high in *cbbM* using enrichments with elevated CO_2 in an attempt to isolate the more ecologically relevant *Zetaproteobacteria*, which have an extremely broad distribution (McAllister et al., 2011).

The reductive tricarboxylic acid (rTCA) cycle represents another major mode of carbon fixation at hydrothermal vents and is effectively a reversal of the TCA cycle. The rTCA cycle enables chemolithoautotophic organisms to convert two molecules of CO_2 to acetyl-CoA. ATP citrate lyase (*aclB*), which catalyzes the ATP-dependent cleavage of citrate to acetyl-CoA and oxaloacetate in a key reaction step, is one of only two enzymes unique to the rTCA cycle (Campbell et al., 2006; Hugler and Sievert, 2011; Nakagawa and Takai, 2008). *M. ferrooxydans* does not have *aclB*, and the rTCA cycle is not thought to be an important contributor to carbon fixation in the *Zetaproteobacteria*. Though it has been hypothesized that *Zetaproteobacteria* primarily fix carbon through the CBB cycle, other

known hydrothermal vent microorganisms, including well-characterized members of the *Epsilonproteobacteria* and *Aquificales*, are known to utilize the rTCA cycle (Beh et al., 1993; Campbell et al., 2008; Hugler et al., 2005; Singer et al., 2011). These organisms have been identified in microbial communities at Loihi and are likely important contributors to carbon fixation there. Relative to *cbbM*, *aclB* was less abundant in our 17 BMS samples (Fig. 3; Fig. 5B/5C), suggesting that, while the gene sequence for *aclB* is present at Loihi, the rTCA cycle may not be as widely used as the CBB cycle. The *Epsilonproteobacteria* and/or the *Zetaproteobacteria* can be considered the most common members of surface microbial mat communities at active seamounts (Emerson and Moyer, 2010). As the rTCA cycle operates in the *Epsilonproteobacteria* and generally at higher temperature deep-sea vents, the large amount of *cbbM* relative to *aclB* supports the hypothesis that, while *aclB* genes are present, *Zetaproteobacteria* and other associated taxa at Loihi's hydrothermal vents use the CBB cycle as their primary means of carbon fixation (Emerson and Moyer, 2010; Hugler and Sievert, 2011; Kato et al., 2013).

Scoop sample PV340 was collected just after the 1996 eruption event at a now dormant hydrothermal venting site known as Jet Vents (T_{max} = 196˚C). At this time, the microbial mats within and around Pele's Pit were characterized by much higher temperatures and sulfur-dependent microbial communities. Jet Vents mats were sampled in 1997 after a major eruption event and had high *aclB*, lower *Zetaproteobacteria*, and low *cbbM* relative to iron-rich samples collected in 2013 (Fig. 5B/5C). Based on T-RFLP data, the Jet Vents community (PV340) also had a very different community than any of the 2013 Loihi iron mats (Fig. 5A). This observation is consistent with well-documented temporal changes in microbial community composition at seamounts and gradual shifts from

Epsilonproteobacteria-dominated communities to *Zetaproteobacteria*-dominated communities as hydrothermal vents cooled over time (Emerson and Moyer, 2010). Loihi 2013 streamer sample (676-BM1-C34) was contained in the T-RFLP cluster (Group 2) nearest PV340 and also had high *aclB*. As *Zetaproteobacteria* depend largely on the CBB cycle for carbon fixation, the presence of *aclB* indicates that these streamer-type mats may be supporting less *Zetaproteobacteria*-impacted microbial communities relative to the other mat types. This idea is supported by *Zetaproteobacteria* abundance data; we found that the Group 1 cluster had an average of 33% *Zetaproteobacteria*, whereas the Group 2 cluster had only 9.1% *Zetaproteobacteria*. The post-eruption microbial mat community from Jet Vents PV340 had only 0.21% *Zetaproteobacteria*, suggesting that percent *Zetaproteobacteria* is inversely associated with *aclB*. These data, in conjunction with the observation that T-RFLP communities are influenced by mat morphology and the statistically significant relationship between *aclB* and mat morphology (univariate ANOVA $p<0.0005$), may indicate that both *Zetaproteobacteria* abundance and *aclB*, representing the *Epsilonproteobacteria*, affect the observed community structure.

Geochemistry data was significantly affected by mat morphology, suggesting that the chemistry of the mat environment is important for determining mat morphology. Fe(II) levels were also significantly described by mat type, and reduced iron availability is likely be important for determining mat morphology. As variance in the abundance of the five target genes was significantly associated with mat type via a one-way MANOVA, Fe(II) may also play a role in variation across functional gene abundance. This is unsurprising given the vital role of iron as an electron donor in the mat habitats at Loihi. QPCR-measured abundances for *cbbM*, *arsC*, *nirK*, and *nifH* were not associated with any independent variable in the

univariate ANOVA, suggesting that these functional genes are not affected by vent temperature or site. Conversely, *aclB* gene copy numbers were significantly affected by mat type, lending additional support to the idea that this gene may be an indicator of community composition. Location of the vents within the caldera is important for some chemical factors, as seen by the significant relationship between sample site and measures of NH_4, NO_x, dSi, and PO_4. This relationship between sample site and vent chemistry was not reflected in the QPCR data. Changes in gene template abundance occur gradually, while chemical changes in the vent environment may happen rapidly. It is also likely that the microorganisms living in these iron-rich habitats are able to function within a range of chemistries that is not extremely variable between our sampling sites. Surprisingly, we did not see an effect of temperature on geochemistry or QPCR data. This is likely due to the relatively narrow temperature range (20-50˚C) of iron-dominated microbial mat communities.

In order to better understand the relationships among functional genes, an NMDS plot was created for log transformed QPCR functional gene data across genes and *Zetaproteobacteria* abundance using a Pearson correlation resemblance matrix (Fig. 4). *nifH* was not included in this analysis. The NMDS analysis grouped *cbbM*, *nirK*, and *arsC* functional genes. These genes were also clustered with *Zetaproteobacteria* abundance indicating that the number of *Zetaproteobacteria* within the mat community may affect the abundance of these functional genes. Both *nirK* and *cbbM* have been identified in PV-1 as well as other uncharacterized strains of *Zetaproteobacteria* (Singer et al., 2011, Singer et al., 2013). Arsenic species have been associated with Fe(III) iron-oxyhydroxides, such as those formed by *Zetaproteobacteria* at Loihi, in both shallow and deep-sea hydrothermal vent systems (Breier et al., 2012; Feely et al., 1991; Pichler et al., 1999). Meyer-Dombard et al.

(2012) found both *arsC* functional genes and *Zetaproteobacteria* SSU rRNA gene sequences in vent fluids and slide colonization experiments in a shallow-sea vent system at Tutum Bay, Papua New Guinea. The rTCA cycle gene *aclB* did not cluster with any other QPCR variable (*arsC*, *nifH*, *nirK*, or *cbbM*). This is unsurprising as it is widely accepted that the rTCA cycle is not associated with *Zetaproteobacteria*, but with other taxa at vents, such as the *Epsilonproteobacteria* (Singer et al., 2011; Beh et al., 1993). It seems likely that while Group 2 *aclB* gene sequence abundances at Loihi may be indicators of mat community structure, they are not associated with *Zetaproteobacteria*-impacted microbial communities, such as those in T-RFLP Group 1. Additional samples from the T-RFLP Group 2 cluster are needed to confirm these hypotheses, as most mat communities analyzed fall into the Group 1 cluster (Fig. 5A).

The identification of *arsC* and *nirK* gene sequences across the fine-scale mat communities assayed here has major implications for the capacity of FeOB communities to participate in denitrification and arsenic detoxification. Amplification of a major *nirK* gene across all samples is notable as the capacity for denitrification may expand the habitat range of *Zetaproteobacteria* or other denitrifying microorganisms in these iron mats. This study represents a first look at arsenic cycling genes at Loihi and opens the door for further investigations into the relationship between chemical arsenic species and the microorganisms living in deep-sea iron-oxidizing communities. Comparison of *cbbM* (CBB cycle) and *aclB* (rTCA cycle) carbon fixation genes revealed that while *cbbM* was ubiquitous in the iron-rich microbial mat habitats, *aclB* was present at appreciable amounts only in the *Epsilonproteobacteria*-rich Jet Vents mat community (PV340) from 1997, along with the T-RFLP Group 2 cluster of iron mat communities from 2013. We conclude that microbial

communities high in *aclB* (T-RFLP Group 2) are likely undergoing the rTCA cycle and may be rich in taxa such as *Aquificales* and/or *Epsilonproteobacteria*. In contrast, T-RFLP Group 1 communities had higher *Zetaproteobacteria* abundance, low *aclB*, and utilize the CBB cycle almost exclusively for carbon fixation. This is also supported by the statistically significant relationship between *aclB* and mat type (univariate ANOVA, $p<0.0005$). Mat morphology was significant with Fe(II) measures in the mats, leading us to hypothesize that reduced iron availability is a forcing function for functional gene abundances, community composition, and mat type.

QPCR can be utilized to efficiently screen large numbers of samples for distinctive functional gene patterns in ecological contexts (Smith and Osborn, 2009). While other molecular studies of functional gene abundance have focused primarily on a single sample or strain, our QPCR approach has enabled the quantitative analysis of gene sequences across a temporal, chemical, morphological, and spatial range of mat samples. The cumulative result of these five QPCR assays is the construction of a unique 'functional gene signature' for discrete, fine-scale microbial mat communities (Fig. 3). These functional gene signatures can be compared across a broad range of environmental parameters and can be used to identify exceptional samples for culturing efforts or additional molecular analyses. To our knowledge, this is the first non-degenerate QPCR approach to the study of functional genes at hydrothermal vents. The five assays we developed can potentially be utilized in the continued study of the functional capacities of iron-dominated hydrothermal systems with regard to carbon and nitrogen fixation, denitrification, and arsenic detoxification. QPCR is a sensitive and valuable molecular tool and is best used in conjunction other assessments and measures, such as the phylogenetic and chemical measures presented here. This study

demonstrates the use of environmentally-derived sequence data to design habitat-specific non-degenerate QPCR analyses, a strategy which can be applied across a variety of microbial communities in a wide range of ecosystems.

Literature Cited

1. Agrawal A, Lal. 2009. Rapid detection and quantification of bisulfite reductase genes in oil field samples using real-time PCR. FEMS Microbiol. Ecol. 69:301-312.
2. Beh M, Strauss G, Huber R, Stetter KO, Fuchs G. 1993. Enzymes of the reductive citric acid cycle in the autotrophic eubacterium *Aquifex pyrophilus* and in the archaebacterium *Thermoproteus neutrophilus*. Arch. Microbiol. 160:306-311.
3. Beller HR, Kane SR, Legler TC, Alvarez PJJ. 2002. A real-time polymerase chain reaction method for monitoring anaerobic hydrocarbon-degrading bacteria based on a catabolic gene. Environ. Sci. Technol. 36:3977-3984.
4. Bothe H, Jost G, Schloter M, Ward BB, Witzel KP. 2000. Molecular analysis of ammonia oxidation and denitrification in natural environments. FEMS Microbiol. Rev. 24 673-690.
5. Braker G, Fesefeldt A, Witzel KP. 1998. Development of PCR primer systems for amplification of nitrite reductase genes (*nirK* and *nirS*) to detect denitrifying bacteria in environmental samples.
6. Braker G, Zhou J, Wu L, Devol AH, Tiedje JM. 2000. Nitrite reductase genes (*nirK* and *nirS*) as functional markers to investigate diversity of denitrifying bacteria in Pacific Northwest marine sediment communities. Appl. Environ. Microbiol. 66:2096-2104.
7. Breier JA, Gomez-Ibanez D, Reddington E, Huber JA, Emerson D. 2012. A precision multi-sampler for deep-sea hydrothermal microbial mat studies. Deep-Sea Res. I 70:83-90.

8. Breier JA., Toner BM, Fakra SC, Marcus MA, White SN, Thurnherr AM, German CR. 2012. Sulfur, sulfides, oxides and organic matter aggregated in submarine hydrothermal plumes at 9 50′ N East Pacific Rise. Geochim. Cosmochim. Acta 88:216-236.
9. Butterfield DA, Jonasson IR, Massoth GJ, Feely RA, Roe KK, Embley RE, Holden JF, McDuff RE, Lilley MD, Delaney JR, Pyle D. 1997. Seafloor eruptions and evolution of hydrothermal fluid chemistry. Phil. Trans. R. Soc. Lond. A 355:369-386.
10. Campbell BJ, Stein JL, Cary SC. 2003. Evidence of chemolithoautotrophy in the bacterial community associated with *Alvinella popejana*, a hydrothermal vent polychaete. Appl. Environ. Microbiol. 69: 5070-5078.
11. Campbell BJ, Engel AS, Porter ML, Takai, K. 2006. The versatile ε-proteobacteria: key players in sulphidic habitats. Nat. Rev. Microbiol. 4:458-468.
12. Chan CS, Fakra SC, Emerson D, Fleming EJ, Edwards KJ. 2011. Lithotrophic iron-oxidizing bacteria produce organic stalks to control mineral growth: implications for biosignature formation. ISME J. 5:717-727.
13. Clarke KR, Gorley RN. 2006. PRIMER v6. Plymouth Marine Laboratory, Plymouth.
14. Druschel GK., Emerson D, Sutka R, Suchecki P, Luther III GW. 2008. Low-oxygen and chemical kinetic constraints on the geochemical niche of neutrophilic iron (II) oxidizing microorganisms. Geochim. Cosmochim. Acta. 72:3358-3370.

15. Dunnebier FK, Becker NC, Caplan-Auerbach J, Clague DA, Cowen J, Cremer M, Garcia M, Goff F, Malahoff A, McMurtry GM, Midson BP, Moyer CL, Norman M, Okubo P, Resing JA, Rhodes JM, Rubin K, Sansone FJ, Smith JR, Spencer K, Wen X, Wheat CG. 1997. Researchers rapidly respond to submarine activity at Loihi volcano, Hawaii. Eos. Trans. AGU 78: 229-233.
16. Emerson D, Moyer CL. 2002. Neutrophilic Fe-oxidizing bacteria are abundant at the Loihi Seamount hydrothermal vents and play a major role in Fe oxide deposition. Appl. Environ. Microbiol. 68:3085-3093.
17. Emerson D, Rentz, JA, Lilburn TG, Davis RE, Aldrich H, Chan C, Moyer CL. 2007. A novel lineage of proteobacteria involved in formation of marine Fe-oxidizing microbial mat communities. PloS One 2:e667.
18. Emerson D, Moyer CL. 2010. Microbiology of seamounts: common patterns observed in community structure. Oceanography 23:148-163.
19. Feely RA, Trefry JH, Massoth GJ, Metz S. 1991. A comparison of the scavenging of phosphorus and arsenic from seawater by hydrothermal iron oxyhydroxides in the Atlantic and Pacific Oceans. Deep-sea Res. 38:617-623.
20. Flemming EJ, Davis RE, McAllister SM, Chan CS, Moyer CL, Tebo BM, Emerson D. 2013. Hidden in plain sight: discovery of sheath-forming, iron-oxidizing *Zetaproteobacteria* at Loihi Seamount, Hawaii, USA. FEMS Microbiol. Ecol. 85:116-127.
21. Gaby JC, Buckley DH. 2012. A comprehensive evaluation of PCR primers used to amplify the *nifH* gene of nitrogenase. PLoS One 7:e42149.

22. Garside C. 1982. A chemiluminescent technique for the determination of nanomolar of nitrate and nitrite in seawater. Mar. Chem. 11: 159-167.

23. Glazer BT, Rouxel OJ. 2009. Redox speciation and distribution within diverse iron-dominated microbial habitats at Loihi Seamount. Geomicrobiol. J. 26:606-622.

24. Grasshoff K, Kremling K, Ehrhardt M. 1999. Methods of Seawater Analysis, 3rd Edition, Wiley-Vch, Weinheim.

25. Hedrich, S, M Schlömann, Johnson DB. The iron-oxidizing proteobacteria. 2011. Microbiology 157:1551-1564.

26. Henry S, Baudoin E, Lopez-Gutierrez JC, Marin-Laurent F, Brauman A, Pilippot L. 2004. Quantification of denitrifying bacteria in soils by *nirK* gene targeted by real-time PCR. J. Microbiol. Methods 59:327-335.

27. Holland HD. 2006. The oxygenation of the atmosphere and oceans. Philos. Trans. R. Soc. Lond. B Biol. Sci. 361:903-915.

28. Holmes RM, Aminot A, Kerouel R, Hooker BA, and Peterson BJ. 1999. A simple and precise method for measuring ammonium in marine and freshwater ecosystems. Can. J. Fish. Aquat. Sci. 56:1801-1808.

29. Hugler M, Wirsen CO, Fuchs G, Taylor CD, Sievert SM. 2005. Evidence for autotrophic CO

30. $_2$ fixation via the reductive tricarboxylic acid cycle by members of the epsilon subdivision of Proteobacteria. J. Bacteriol. 187:3020-3027.

31. Hugler M, Sievert, SM. 2011. Beyond the Calvin cycle: autotrophic carbon fixation in the ocean. Ann. Rev. Mar. Sci. 3:261-289.

32. Jackson CR, Dugas SL. 2003. Phylogenetic analysis of bacterial and archaeal *arsC* gene sequences suggests an ancient, common origin for arsenate reductase. BMC Evol. Biol. 3:18.

33. Jannasch HW, and Mottl MJ. 1985. Geomicrobiology of deep-sea hydrothermal vents. Science 229:717-725.

34. Kato SK, Nakawake M, Ohkuma M, Yamagishi A. 2012. Distribution and phylogenetic diversity of cbbM genes encoding rubisCO form II in a deep-sea hydrothermal field revealed by newly designed primers. Extremophiles 16: 277-283.

35. Kikuchi T, Iwasaki K, Nishihara H, Takamura Y, Yagi O. 2002. Quantitative and rapid detection of the trichloroethylene-degrading bacterium *Methylocyctis* sp. M in groundwater by real-time PCR. Appl. Microbiol. Biotechnol. 59:731-736.

36. Ludwig W, Strunk O, Westram R, et al. 2004. ARB: a software environment for sequence data. Nucl. Acids Res. 32:1363-1371.

37. McAllister SM, Davis RE, McBeth JM, Tebo BM, Emerson D, Moyer CL. 2011. Biodiversity and emerging biogeography of the neutrophilic iron-oxidizing *Zetaproteobacteria*. Appl. Environ. Microbiol. 77:5445-5457.

38. Mehta MP, Butterfield DA, Baross JA. 2003. Phylogenetic diversity of nitrogenase (*nifH*) genes in deep-sea and hydrothermal vent environments of the Juan de Fuca Ridge. Appl. Environ. Microbiol. 69:960-970.

39. Meyer F, Paarmann D, D'Souza M, Olson R, Glass EM, Kubal M, Paczian T, Rodriguez A, Stevens R, Wilke A, Wilkening J, Edwards RA. 2008. The metagenomics RAST server-a public resource for the automatic phylogenetic and functional analysis of metagenomes. BMC Bioinformatics 9: 386.

40. Meyer-Dombard DR, Amend JP, Osburn MR. 2012. Microbial diversity and potential for arsenic and iron biogeochemical cycling at an arsenic rich, shallow-sea hydrothermal vent (Tutum Bay, Papua New Guinea). Chem. Geol. 348:37-47.
41. Minic, Z, Thongbam PD. 2011. The biological deep-sea hydrothermal vent as a model to study carbon dioxide capturing enzymes. Marine Drugs *9*:719-738.
42. Moyer CL. 2001.Molecular phylogeny: applications and implications for marine microbiology. Methods Microbiol. 30:375-394.
43. Mukhopadhyay R, Rosen BP. 2002. Arsenate reductases in prokaryotes and eukaryotes. Environ. Health Perspect. 110:745-748.
44. Nakagawa S, Takai K. 2008. Deep-sea vent chemoautotrophs: diversity, biochemistry and ecological significance. FEMS Microbial Ecol. 65:1-14.
45. Namiki T, Hachiya T, Tanaka H, Sakakibara Y. 2012. MetaVelvet: an extension of Velvet assembler to *de novo* metagenome assembly from short sequence reads. Nucl. Acids Res. 40: e155.
46. Pichler T, Veizer J, Hall GEM. 1999. Natural input of arsenic into a coral-reef ecosystem by hydrothermal fluids and its removal by Fe(III) oxyhydroxides. Environ. Sci. Technol. 33:1373-1378.
47. Pruesse E, Quast C, Knittel K, Fuchs BM, Ludwig W, Peplies J, Glockner FO. 2007. SILVA: a comprehensive online resource for quality checked and aligned ribosomal RNA sequence. Nucl. Acids Res. 35:7188-7196.
48. Rose TM, Schultz ER, Henikoff JG, Pietrokovski S, McCallum CM, Henikoff S. 1998. Consensus-degenerate hybrid oligonucleotide primers for amplification of distantly related species. Nucl. Acids Res. 26:1628-1635.

49. Rassa AC, McAllister SM, Safran SA, Moyer CL. 2009. *Zeta-Proteobacteria* dominate the colonization and formation of microbial mats in low-temperature hydrothermal vents at Loihi Seamount, Hawaii. Geomicrobiol. J. 26:623-638.

50. Ritalahti KM, Amos BK, Youlboong S, Qingzhong W, Koenigsberg SS, Lofflerr FE. 2006. Quantitative PCR targeting 16S rRNA and reductive dehalogenase genes simultaneously monitors multiple *dehalococcoides* strains. Appl. Envir. Microbiol. 72:2765-2774.

51. Sakai H, Tsubota H, Nakai T, Ishibashi J, Akagi T, Gamo T, Tilbrook B, Igarashi G, Kodera M, Shitashima K, Nakamura S, Fujboka K, Watanabe M, McMurtry G, Malahoff A, Ozima, M. 1987. Hydrothermal activity on the summit of Loihi Seamount, Hawaii. Geochem. J. 21.1:11-21.

52. Sonia H, Baudoin E, Lopez-Gutierrez JC, Martin-Laurent F, Brauman A, Philippot L. 2004. Quantification of denitrifying bacteria in soils by *nirK* gene targeted real-time PCR. J. Microbiol. Methods 59:327-335.

53. Shively JM, van Keulen G, Meijer WG. 1998. Something from almost nothing: carbon dioxide fixation in chemoautotrophs. Ann. Rev. Microbiol. 52:191-230.

54. Singer E, Emerson D, Webb EA, Barco RA, Kuenen JG, Nelson WC, Chan CS, Comolli LR, Ferriera S, Johnson J, Heidelberg JF, Edwards KJ. 2011. *Mariprofundus ferrooxydans* PV-1 the first genome of a marine Fe(II) oxidizing *Zetaproteobacterium*. PLOS One 6:1-9.

55. Singer E, Heidelberg JF, Dhillon A, Edwards KJ. 2013. Metagenomic insights into the dominant Fe(II) oxidizing *Zetaproteobacteria* from an iron mat at Loihi, Hawaii. Front. Microbiol. 4:1-9.

56. Smith GB, JM Tiedje. 1992. Isolation and characterization of a nitrite reductase gene and its use as a probe for denitrifying bacteria. Appl. Environ. Microbiol. 58:376-384.
57. Soblev D, Roden EE. 2004. Characterization of a neutrophilic, chemolithoautotrophic Fe(II)-oxidizing β-proteobacterium from freshwater wetland sediments. Geomicrobiol. J. 21:1-10.
58. Stookey LL. 1970. Ferrozine- a new spectrophotometric reagent for iron. Analyt. Chem. 42:779-781.
59. Tabita RF, Hanson TE, Li H, Stagopan S, Singh J, Chan S. 2007. Function, structure, and evolution of the RubisCO-like proteins and their RubisCO-like homologs. Microbiol. Mol. Biol. Rev. 71:575-599.
60. Tang Y, Shigematsu T, Morimura IS, Kida K. 2004. The effects of micro-aeration on the phylogenetic diversity of microorganisms in a thermophilic anaerobic municipal solid-waste digester. Water Res. 38:2537-2550.
61. Von Damm KL, Edmond JM, Measures CI, Walden B, Weiss RF. 1985. Chemistry of submarine hydrothermal solutions at 21° N, East Pacific Rise. Geochim. Cosmochim. Acta 49:2197-2220.
62. Wang F, Zhou H, Meng J, Peng X, Jiang L, Sun P, Zhang C, Van Nostrand J, Deng Y, Wu L, Zhou J, Xiao X. 2009. GeoChip-based analysis of metabolic diversity of microbial communities at the Juan de Fuca Ridge hydrothermal vent. Proc. Nat. Acad. Sci. 106:4840-4845.
63. Weber KA, Achenbach LA, Coates JD. 2006. Microorganisms pumping iron: anaerobic microbial iron oxidation and reduction. Nat. Rev. Micro. 4:752-764.

64. Wheat CG, Jannasch HW, Plant JN, Moyer CL, Sanson FJ, McMurty GM. 2000. Continuous sampling of hydrothermal fluids from Loihi Seamount after the 1996 event. J. Geophys. Res. 105:19,353-19,367.

65. Xie W, Wang F, Guo L, Chen Z, Sievert SM, Meng J, Huang G, Li Y, Yan Q, Wu S, Wang X, Shangwu C, Guangyuan H, Xiao X, Xu A. 2011. Comparative metagenomics of microbial communities inhabiting deep-sea hydrothermal vent chimneys with contrasting chemistries. ISME J. 5:414-426.

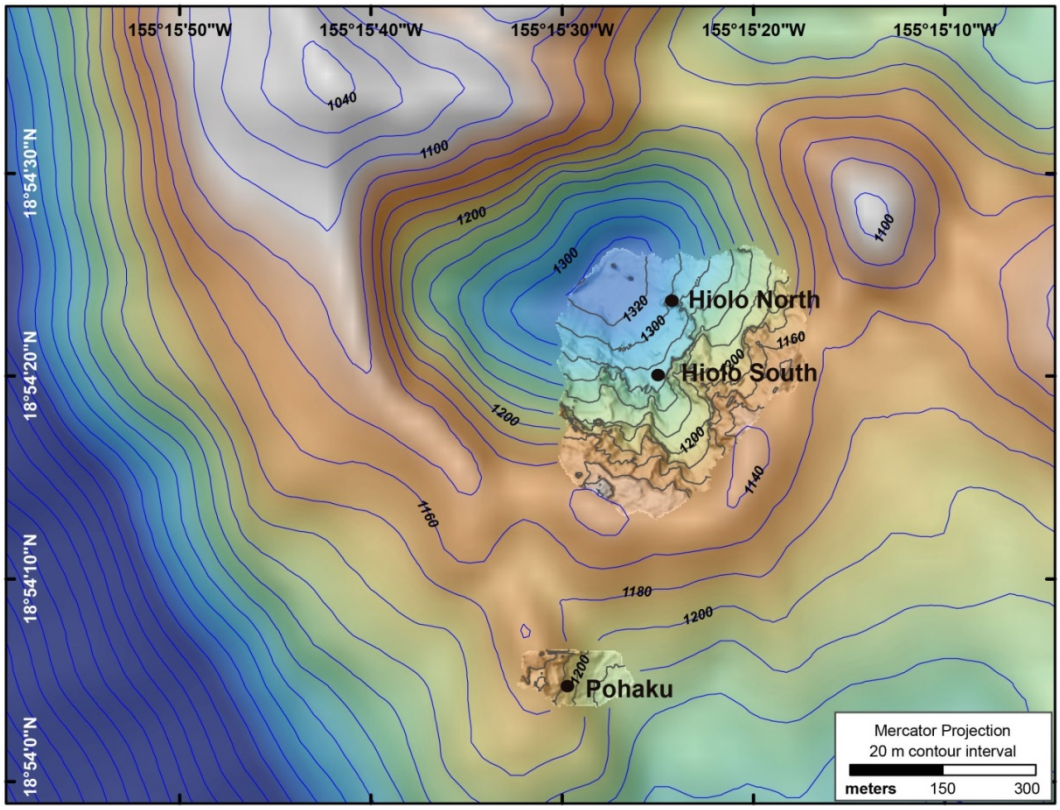

Fig. 1: Bathymetric map of sampling sites in Pele's Pit at Loihi Seamount, HI.

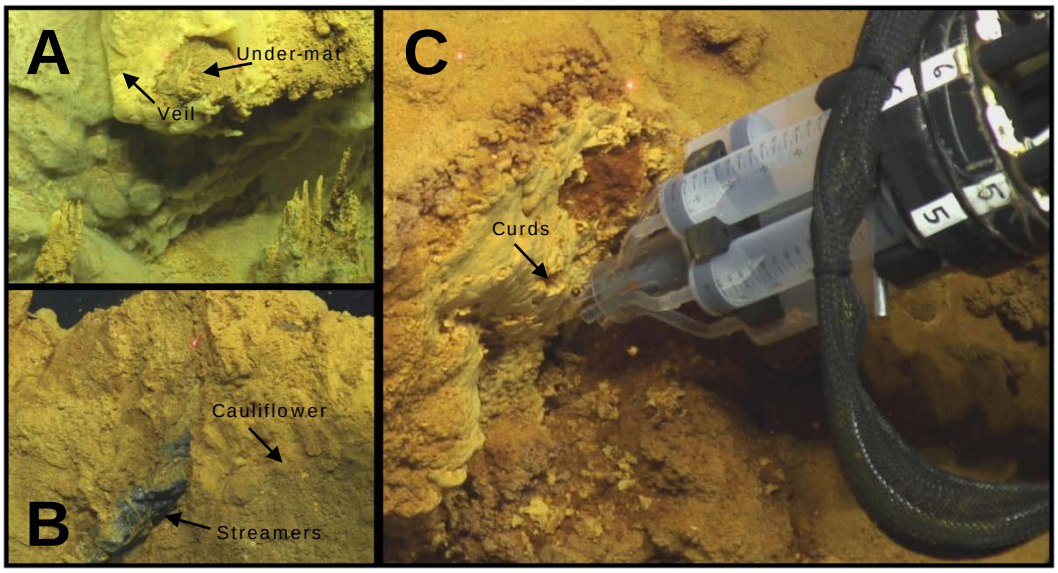

Fig. 2: Microbial iron mats at Loihi Seamount, HI formed by *Zetaproteobacteria* during the oxidation of Fe(II) to insoluble Fe(III) oxyhydroxides at circumneutral pH. Distance between lasers is 10 cm. (A) Iron mats formed over venting chimneys at Hiolo North. The light-colored top layer of the mat, termed 'veil', has peeled back revealing the 'under-mat'. (B) 'Cauliflower' iron mats surrounding an actively venting orifice at Hiolo South. Filamentous 'streamers' are also visible in the orifice. (C) The biomat syringe (BMS) sampler operated by the *ROV Jason II* sampling a 'curd'-like mat layer at Pohaku.

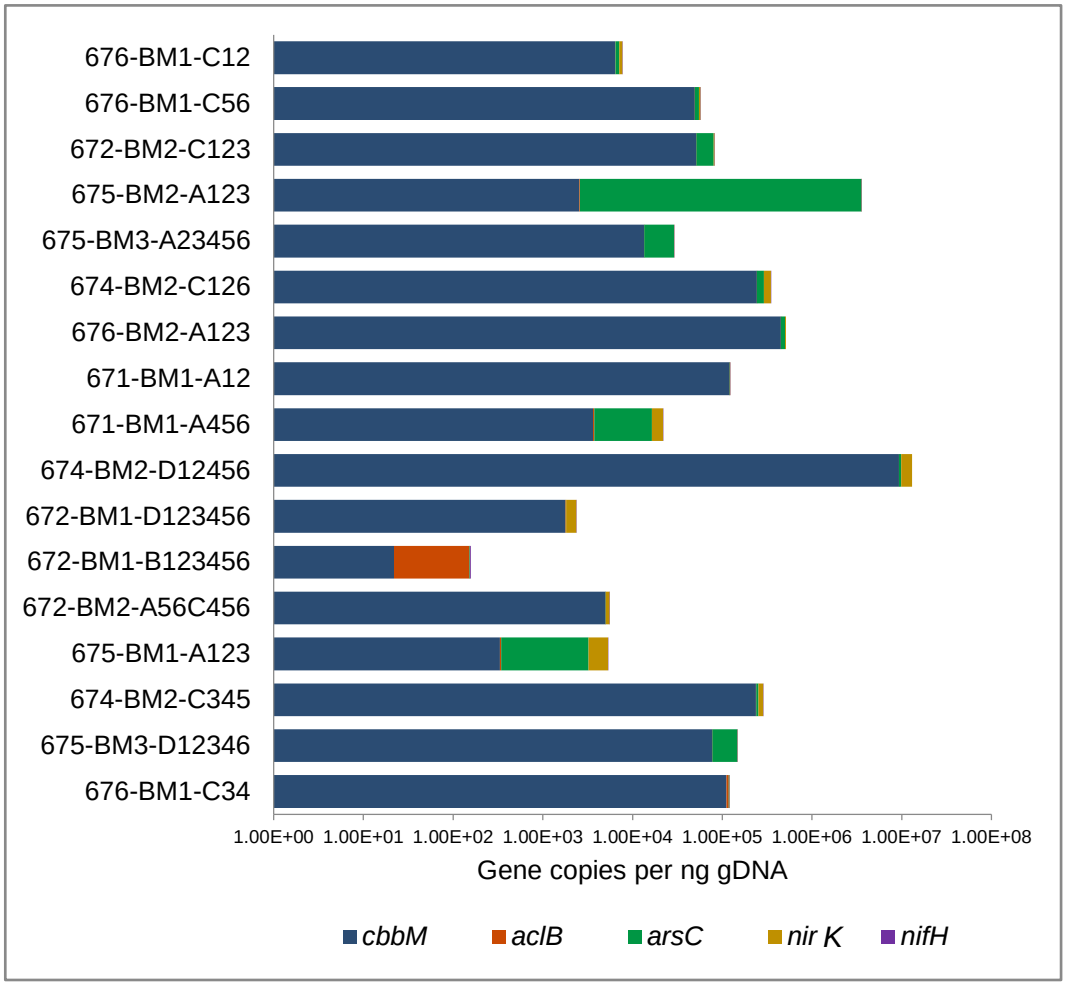

Fig. 3: Stacked bar graphs showing functional gene copy numbers by QPCR for *cbbM*, *aclB*, *arsC*, *nirK*, and *nifH* for 17 BMS samples collected at Loihi in 2013. Functional gene copy numbers are represented on a logarithmic y-axis. See FIG. S1 for linear representation of this data.

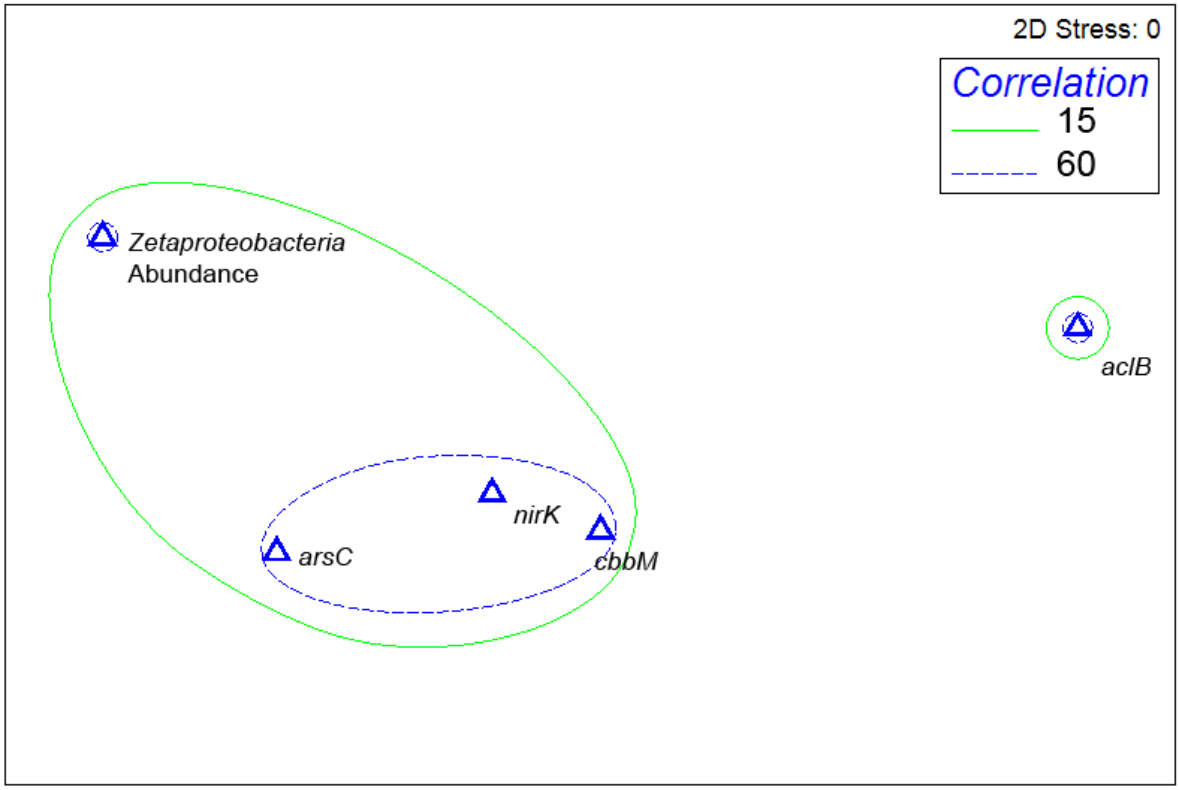

Fig. 4: Pearson correlation non-parametric multidimensional scaling (NMDS) plot generated using a group average resemblance matrix of log-transformed functional gene and *Zetaproteobacteria* abundance QPCR data for 17 BMS samples. Contours indicate clusters with 15 and 60 percent Pearson correlation.

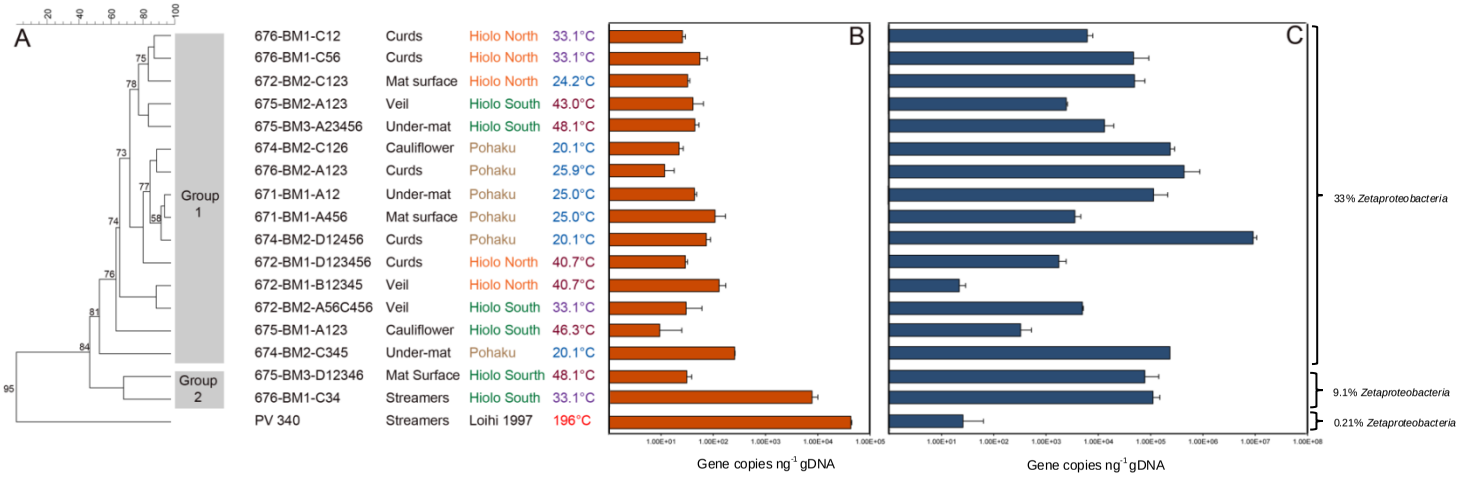

Fig. 5: (A) Group-average cluster analysis of T-RFLP DNA fingerprints from 17 Loihi BMS samples. PV340, a 1997 scoop sample taken shortly after a major eruption event at Loihi, is included for comparison. Values at nodes are cophenetic correlation coefficients. (B) Bar graph showing *aclB* gene copy numbers. (C) Bar graph showing *cbbM* gene copy numbers. Error bars represent standard error across triplicate QPCR reactions. Functional gene copy numbers are represented on a logarithmic y-axis. See FIG S2 for a linear representation of QPCR data. Average percent *Zetaproteobacteria* values were calculated for across all samples in any given T-RFLP Group.

TABLE 1. Summary of functional gene QPCR primers.

Gene	Function	Primer names	Primer sequences 5'-3'	Sequence source	Annealing temp.
Nitrogenase (*nifH*)	Nitrogen fixation	nifH5F/ nifH5R	GGTAAATCCACTACTACCCAGAA/ GAAGGATCAGACGTGTGGAA	Soda Bay, Alaska metagenomic assembly	55˚C
Nitrite reductase (*nirK*)	Denitrification	nir2F/ nir2R	CGTGCGATAATACGGTGAT/ CCTTCTGCCAATGGTCCTT	Loihi, Hawaii metagenomic assembly	60˚C
Arsenate reductase (*arsC*)	Arsenic detoxification	arsC2F/ arsC2R	GCGTACAGGCGAAGATGAATA/ ACAACAACAGGACGTCAA	Loihi, Hawaii metagenomic assembly	60˚C
ATP citrate lyase (*aclB*)	Carbon fixation via rTCA cycle	aclB3F/ aclB3R	GCTTTGGCAAATGGTTCAGG/ ACCGACTTCTGGAAAGTATTGG	Amplified with primers from Campbell et al. (2003)	53˚C
RuBisCO type II (*cbbM*)	Carbon fixation via CBB cycle	cbbM7.3F/ cbbM7.3R	GCTTTGGCAAATGGTTCAGG/ ACCGACTTCTGGAAAGTATTGG	Amplified with primers from Kato et al. (2013)	60˚C

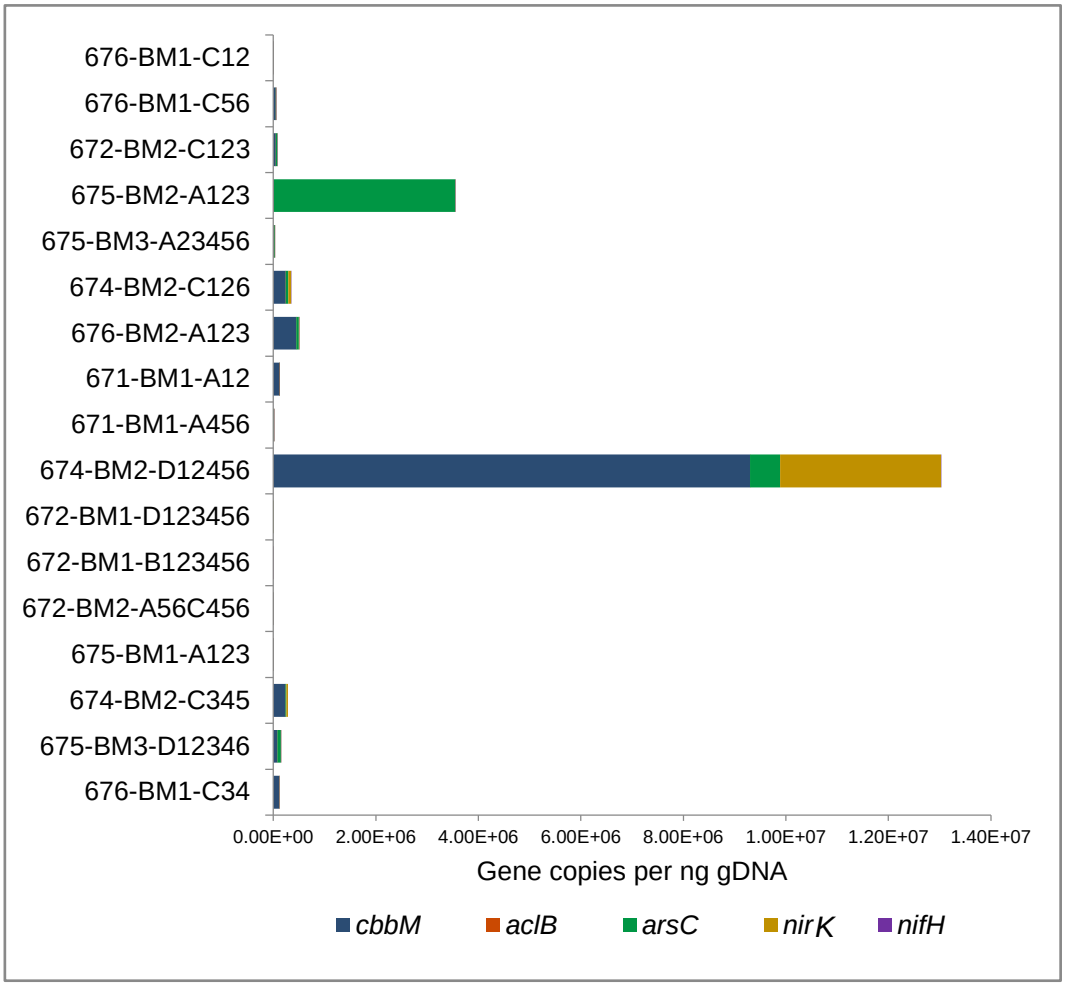

Fig. S1: Stacked bar graphs plotted on a linear scale showing functional gene copy numbers by QPCR for *cbbM*, *aclB*, *arsC*, *nirK*, and *nifH*.

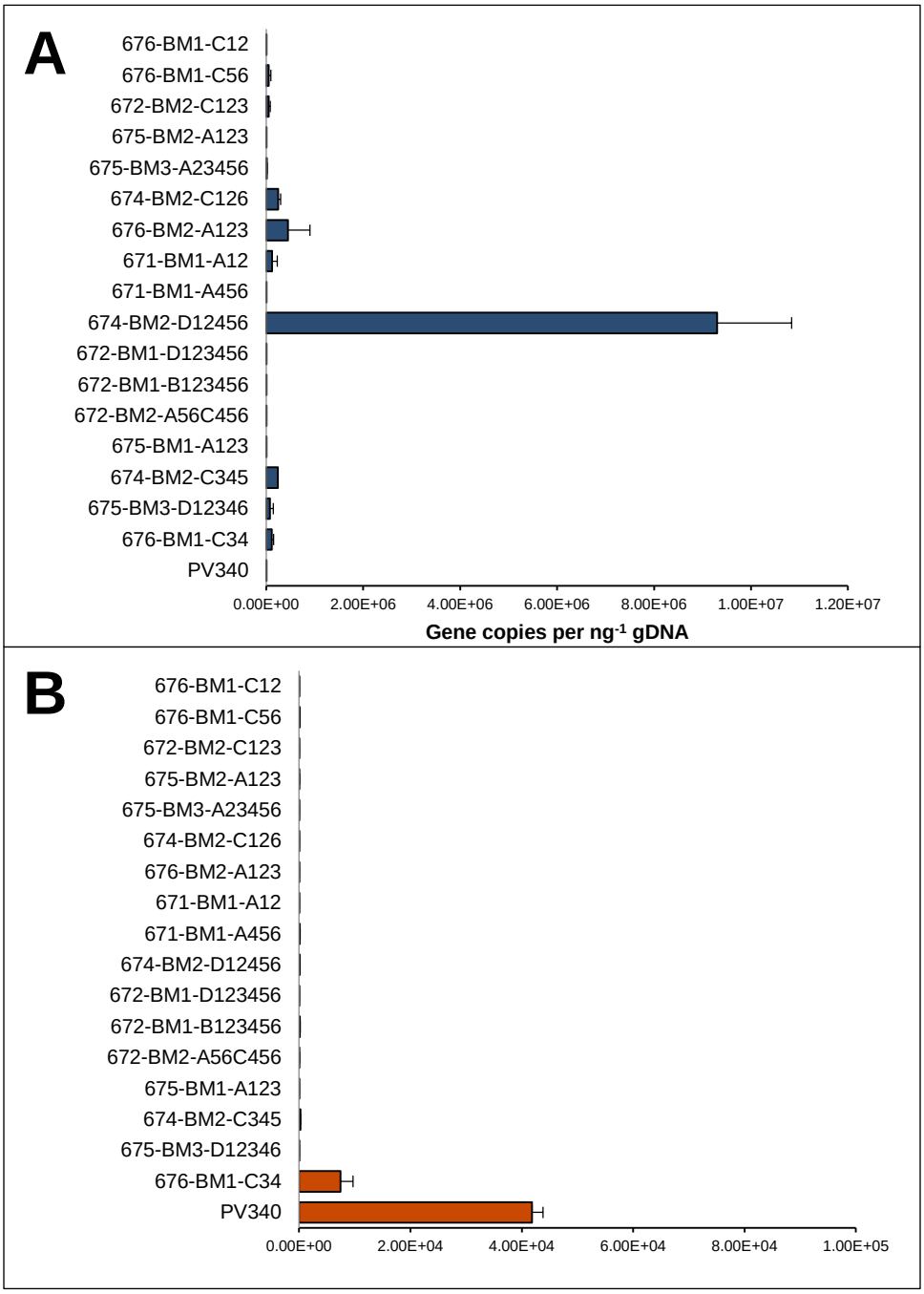

Fig. S2: Bar graphs plotted on a linear scale showing functional gene copy numbers by QPCR for (A) *cbbM* and (B) *aclB*.

TABLE S1. Chemical measurements for BMS samples taken at Loihi Seamount.

Site	Sample	Temp.	Gross mat morphology	NH_4^+ (µM)	NO_2^- (µM)	NO_x µM)	dSi (µM)	PO_4 (µM)	Fe(II) (µM)
Pohaku	671-BM1-A12	25.9°C	Under-mat	4.211	0.333	17.70	160.6	3.209	166
Pohaku	671-BM1-A456	25.9°C	Mat surface	4.235	0.124	30.01	210.6	0.448	101
Pohaku	676-BM2-A123	25.6°C	Curds	2.096	0	4.020	456.6	3.761	ND
Hiolo South	675-BM1-A123	46.3°C	Cauliflower	1.925	0.215	4.528	700.6	6.215	42.3
Hiolo South	675-BM1-A456	46.3°C	Cauliflower	1.925	0.215	4.528	700.6	6.215	20.0
Hiolo South	675-BM1-B123456	47.4°C	Veil	1.925	0.215	4.528	700.6	6.215	0
Hiolo South	675-BM2-A123	43.0°C	Veil	2.528	0	2.789	477.6	6.521	11.0
Hiolo South	675-BM2-A456	43.0°C	Cauliflower	2.528	0	2.789	477.6	6.521	118
Hiolo South	675-BM3-A23456	48.1°C	Under-mat	1.925	0.215	4.528	700.6	6.215	232
Hiolo South	675-BM3-D12346	48.1°C	Mat surface	1.925	0.215	4.528	700.6	6.215	180
Hiolo North	676-BM1-C12	33.0°C	Curds	3.032	0.236	11.82	352.6	2.718	0
Hiolo North	676-BM1-C34	33.0°C	Streamers	3.032	0.236	11.82	352.6	2.718	46.2
Hiolo North	676-BM1-C56	33.0°C	Curds	3.032	0.236	11.82	352.6	2.718	18.3
Hiolo North	672-BM1-B123456	40.7°C	Veil	2.096	0.093	1.859	218.6	3.699	0